© 2018. Published by The Company of Biologists Ltd | Journal of Cell Science (2018) 131, jcs214379. doi:10.1242/jcs.214379

SHORT REPORT

CCAR-1 affects hemidesmosome biogenesis by regulating *unc-52*/perlecan alternative splicing in the *C. elegans* epidermis

Rong Fu[1], Yi Zhu[1], Xiaowan Jiang[1], Yuanbao Li[1], Ming Zhu[2], Mengqiu Dong[2], Zhaohui Huang[1], Chunxia Wang[1], Michel Labouesse[3] and Huimin Zhang[1,*]

ABSTRACT

Hemidesmosomes are epithelial-specific attachment structures that maintain tissue integrity and resist tension. Despite their importance, how hemidesmosomes are regulated at the post-transcriptional level is poorly understood. *Caenorhabditis elegans* hemidesmosomes (CeHDs) have a similar structure and composition to their mammalian counterparts, making *C. elegans* an ideal model for studying hemidesmosomes. Here, we focus on the transcription regulator CCAR-1, identified in a previous genetic screen searching for enhancers of mutations in the conserved hemidesmosome component VAB-10A (known as plectin in mammals). Loss of CCAR-1 function in a *vab-10(e698)* background results in CeHD disruption and muscle detachment from the epidermis. CCAR-1 regulates CeHD biogenesis, not by controlling the transcription of CeHD-related genes, but by affecting the alternative splicing of *unc-52* (known as perlecan or HSPG2 in mammals), the predicted basement extracellular matrix (ECM) ligand of CeHDs. CCAR-1 physically interacts with HRP-2 (hnRNPR in mammals), a splicing factor known to mediate *unc-52* alternative splicing to control the proportions of different UNC-52 isoforms and stabilize CeHDs. Our discovery underlines the importance of post-transcriptional regulation in hemidesmosome reorganization. It also uncovers previously unappreciated roles of CCAR-1 in alternative splicing and hemidesmosome biogenesis, shedding new light on the mechanisms through which mammalian CCAR1 functions in tumorigenesis.

KEY WORDS: Hemidesmosome, CCAR1, Alternative splicing, *unc-52*, Perlecan, *C. elegans*

INTRODUCTION

Hemidesmosomes are epithelial-specific adhesion structures connecting intermediate filaments to the extracellular matrix (ECM) (Litjens et al., 2006). The primary function of hemidesmosomes is to maintain tissue integrity and resist tension, but also to participate in physiological or pathological processes such as mechanotransduction, immune regulation and tumor progression (De Arcangelis et al., 2016; Laval et al., 2014; Zhang et al., 2011; Zhang et al., 2015). *Caenorhabditis elegans* hemidesmosomes (CeHDs) are structurally and functionally analogous to vertebrate type I hemidesmosomes. VAB-10A is the *C. elegans* counterpart of mammalian plectin in hemidesmosomes and serves as the core CeHD component to link intermediate filaments (composed of IFA-2, IFA-3 and IFB-1) with apical and basal transmembrane proteins (MUP-4 and LET-805, respectively), anchoring the epidermis to the cuticle and muscles (Bosher et al., 2003). To better understand how CeHDs function, we previously performed a genome-wide RNAi screen searching for enhancers of a viable *vab-10A(e698)* allele with a missense mutation in the plectin repeats of VAB-10A. Among the candidates, we identified *ccar-1* (cell cycle and apoptosis regulator 1, previously known as *lst-3* or *sup-38*) as a gene essential for hemidesmosome maturation in the *vab-10A(e698)* background (Zahreddine et al., 2010).

Mammalian CCAR1 is a well-known regulator of cell growth and apoptosis. The fact that CCAR1 promotes the growth of several cancer types suggests that *CCAR1* acts as an oncogene (Ha et al., 2016; Muthu et al., 2015; Ou et al., 2009). CCAR1 functions mainly by binding to transcription regulators, such as estrogen receptor α, p53, β-catenin and neurogenin-3. Through different protein–protein interactions, CCAR1 can activate multiple downstream targets implicated in proliferation, apoptosis and differentiation (Kim et al., 2008; Lu et al., 2012; Ou et al., 2009). CCAR1 possesses a DNA-binding domain, a RNA-binding domain and several protein interaction domains, indicating that CCAR1 might participate in multiple processes (Brunquell et al., 2014). However, functions of CCAR1 in processes other than transcriptional regulation still remain undiscovered. *C. elegans* CCAR-1 is highly similar to mammalian CCAR1 (Fig. S1). In this work, we carry out detailed analysis to evaluate the function and mechanism of CCAR-1 in CeHD organization. Our study reveals that CCAR-1 affects CeHD biogenesis, not through transcriptional regulation, but by working together with splicing factors to control the alternative splicing of the basement membrane component UNC-52 (known as perlecan or HSPG2 in mammals). These results implicate CCAR1 in a new role in hemidesmosome biogenesis and splicing regulation.

RESULTS AND DISCUSSION

Loss of CCAR-1 function affects CeHD integrity during embryonic development

To confirm the result obtained from our RNAi screen, we constructed a *vab-10A(e698); ccar-1(gk433)* double mutant for detailed examination. The *ccar-1*-null allele *gk433* combined with *vab-10A(e698)* greatly increased the lethality and morphological defects over that seen in single mutants (Fig. 1). Antibody staining of the *vab-10A(e698); ccar-1(gk433)* embryos revealed clear muscle detachment from the outer body wall, which is characteristic of compromised CeHD integrity (Fig. 1A, arrows) (Bosher et al., 2003; Zahreddine et al., 2010; Zhang et al., 2011). The muscle-detachment defect was also obvious in the surviving L1 double-mutant larvae, but was not found in *ccar-1(gk433)* or *vab-*

[1]Jiangsu Key Laboratory of Infection and Immunity, Institutes of Biology and Medical Sciences, Soochow University, Suzhou 215123, China. [2]National Institute of Biological Sciences, Beijing 102206, China. [3]Institut de Biologie Paris Seine, Université Pierre et Marie Curie, Paris 75005, France.

*Author for correspondence (zhanghuimin@suda.edu.cn)

H.Z., 0000-0002-2167-9644

Received 21 December 2017; Accepted 2 May 2018

Journal of Cell Science (2018) 131, jcs214379. doi:10.1242/jcs.214379

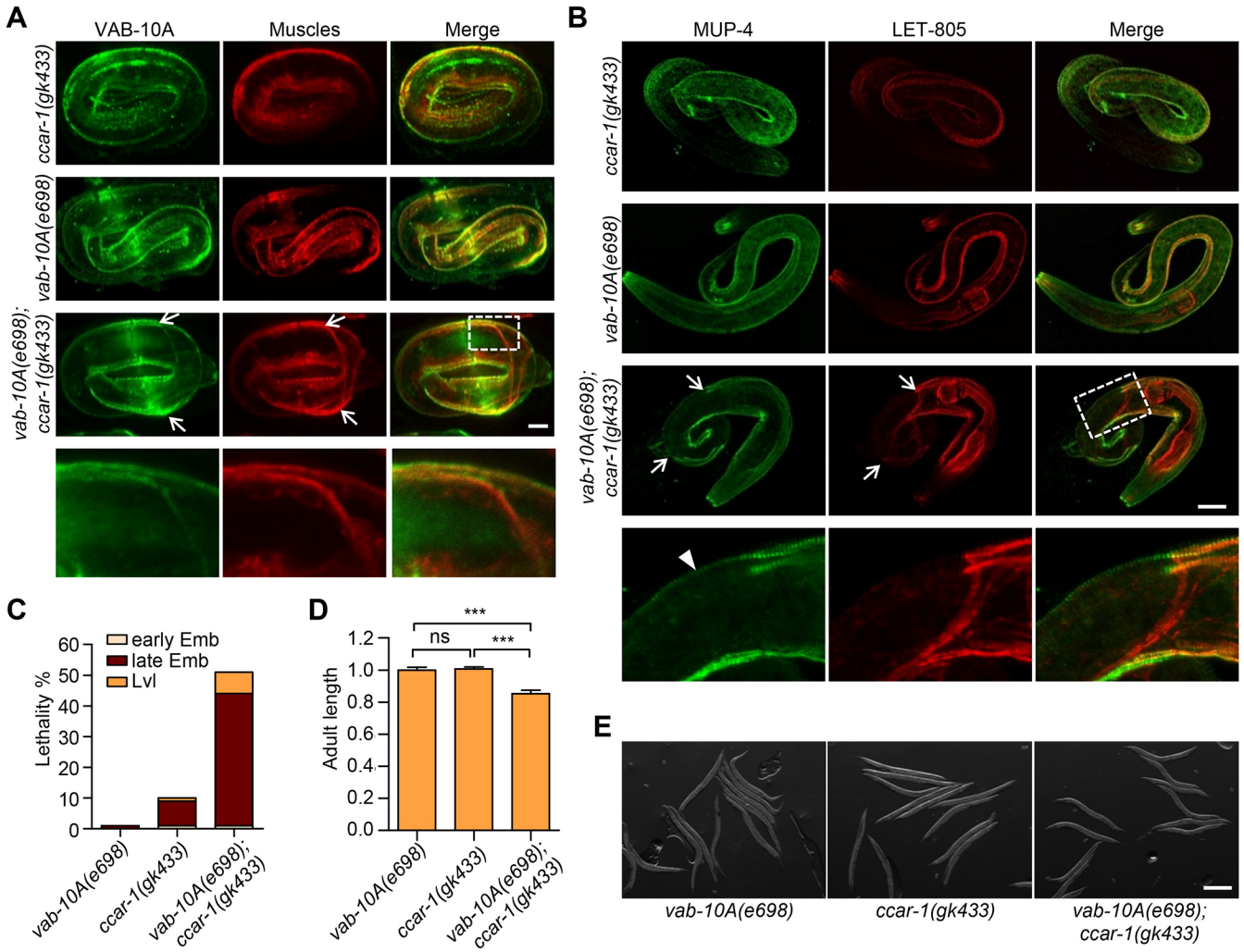

Fig. 1. Loss of CCAR-1 function affects CeHD integrity. (A) PAT-3 (muscle-specific; red) and VAB-10A (green) immunostaining of embryos at the three-fold elongation stage. Scale bar: 5 µm. (B) LET-805 (basal CeHDs; red) and MUP-4 (apical CeHDs; green) immunostaining of L1 larvae. Scale bar: 20 µm Arrows in A and B are detached muscles. Arrowhead, apical CeHDs. Boxed areas in A and B are enlarged in the lower panel. (C) Lethality of mutants arrested at different development stages (2 biological replicates, $n \geq 155$/genotype). Early emb, embryonic lethality before elongation; late emb, embryonic lethality during or post elongation; lvl, larval lethality. (D,E) Bright-field images and body length measurements of adult animals. Results in D are mean±s.e.m. ($n \geq 31$/genotype). ***$P<0.001$; ns, not significant (two-tailed unpaired *t*-test). Scale bar: 300 µm.

10A(e698) single mutants (Fig. 1A,B). Double-staining of MUP-4 and LET-805 (markers for apical and basal CeHDs, respectively) showed that the detachment happened at the basal side of the epidermal cells, whereas the apical CeHDs remained relatively unaffected (Fig. 1B). Consistent with the muscle-detachment phenotype, ∼50% of double mutants died before or soon after hatching, with more than 40% arrested during embryonic elongation when CeHDs undergo extensive reorganization (Fig. 1C). The *vab-10A(e698);ccar-1(gk433)* individuals that survived into adulthood exhibited no additional morphological defects except a slightly shortened body (Fig. 1D,E). These results suggest that CCAR-1 functions together with VAB-10A to maintain CeHD integrity during embryonic and early larval development.

CCAR-1A is the major isoform responsible for CeHD biogenesis in the epidermis

The *C. elegans ccar-1* locus generates four isoforms (denoted A–D), as predicted by wormbase and confirmed by RT-PCR experiments (Fig. 2A). To clarify which isoform is required for maintaining CeHD integrity, we performed targeted deletion and isoform-specific rescue experiments. First, we created a loss-of-function allele *ccar-1(sda11)*, which contains a 13 bp deletion in exon 7 of *ccar-1* and presumably causes a frameshift at amino acid number 1007, which is located in the C-terminus of CCAR-1A. *vab-10A(e698)* combined with *ccar-1(sda11)* resulted in a similar degree of lethality to that of *vab-10A(e698);ccar-1(gk433)* double mutants (Fig. 2B). Second, expressing CCAR-1A alone rescued the lethality of *vab-10A(e698); ccar-1(gk433)* as efficiently as using the *ccar-1* genomic sequence, which mediates expression of all isoforms (Fig. 2B). Based on the above evidence, we conclude that CCAR-1A is the major isoform responsible for maintaining CeHD integrity. It is worth noting that among the four CCAR-1 isoforms, CCAR-1A is the most similar to human CCAR1. The primary functional domains of human CCAR1, namely the S1-like domain, the deleted in breast cancer 1 (DBC1) domain and the SAF-A/B, Acinus and PIAS (SAP) domain, can all be found in *C. elegans* CCAR-1A (Fig. 2A).

To determine the expression pattern of CCAR-1A, a translational CCAR-1A::GFP fusion was created. Confocal images showed that

Journal of Cell Science (2018) 131, jcs214379. doi:10.1242/jcs.214379

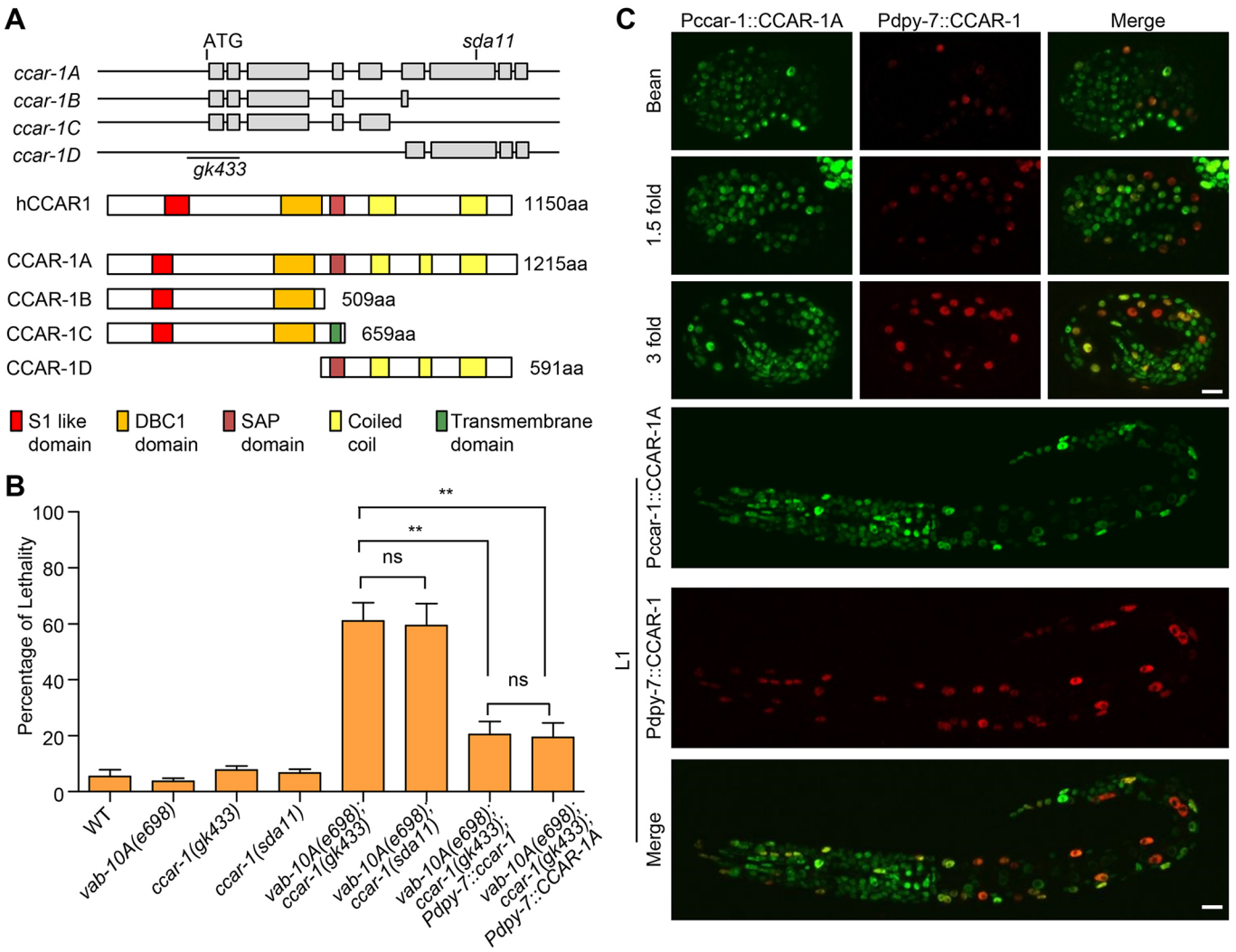

Fig. 2. CCAR-1A is the major isoform responsible for CeHD biogenesis in the epidermis. (A) Diagrams of the *ccar-1* locus and the conserved domains of CCAR-1 isoforms compared with human CCAR1 (hCCAR1). The location of *gk433* (933 bp deletion) and *sda11* (13 bp deletion plus frameshift) mutations are indicated. (B) Lethality of single and double mutants, as well as the *vab-10A(e698); ccar-1(gk433)* double mutant rescued by all CCAR-1 isoforms or CCAR-1A expressed solely in the epidermis. Results are mean±s.e.m. (three biological replicates, $n \geq 81$/condition). $^{**}P<0.01$; ns, not significant (two-tailed, unpaired *t*-test). WT, wild type. (C) Distribution of CCAR-1A (Pccar-1::CCAR-1A) in epidermal cells (marked by Pdpy-7::CCAR-1::mCherry) at embryonic (bean, 1.5 fold, three-fold) stages and L1 larvae. Scale bars: 5 µm for embryos, 10 µm for larvae.

CCAR-1A was localized in the nuclei of most cells at various developmental stages (Fig. 2C). To examine whether CCAR-1A is expressed in all epidermal cells, we generated an epidermal-specific CCAR-1::mCherry transgene controlled by the *dpy-7* promoter. Colocalization analysis showed that every nucleus of the epidermis marked by Pdpy-7::CCAR-1::mCherry was also positive for CCAR-1A::GFP driven by the *ccar-1* promoter (Fig. 2C). This observation is consistent with results showing that restoring CCAR-1A expression in the epidermis alone was sufficient to rescue the lethality of *vab-10A(e698);ccar-1(gk433)* mutants (Fig. 2B). These data together suggest that CCAR-1A primarily functions in the epidermal cells to maintain CeHDs during *C. elegans* development.

CCAR-1 maintains CeHD integrity by regulating *unc-52* alternative splicing

The mammalian homolog of CCAR-1 is a well-known transcriptional regulator (Kim et al., 2008; Muthu et al., 2015). Therefore, to determine the molecular targets of CCAR-1 in CeHDs, we first tested whether the expression of any CeHD-related gene is affected by CCAR-1 in embryos by performing an microarray analysis (Tables S1,S2). Table S1 summarizes the transcriptional changes of all the known CeHD components and regulators after *ccar-1* inactivation. The results showed that there was no significant change in the transcription of any CeHD-related gene in *ccar-1(gk433)* mutant embryos compared with wild type (Table S1). A quantitative real-time PCR (QPCR) analysis also confirmed that the transcription of CeHD-related components was not affected by loss of *ccar-1* (Fig. 3A). These data suggest that CCAR-1 does not regulate CeHD biogenesis by controlling the transcription of CeHD-related genes. We then performed genetic-interaction analysis to explore the functional links between CCAR-1 and CeHD-related components. Interestingly, UNC-52/perlecan, the major basement ECM ligand of CeHDs, stood out among the CeHD-related components tested. Treating *ccar-1(gk433)* with *unc-52* RNAi enhanced embryonic lethality to up to 100%, and caused muscle detachment, similar to what was observed in *vab-10A(e698);ccar-1(gk433)* embryos (Fig. 3B,C).

Journal of Cell Science (2018) 131, jcs214379. doi:10.1242/jcs.214379

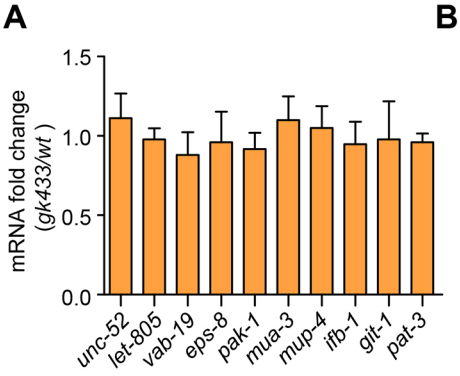

B

Gene	Lethality (20 ℃)	
	WT	*ccar-1(gk433)*
mua-3	1.4% (n=212)	2.6% (n=156)
mup-4	100% (n=129)	83% (n=127)
let-805	100% (n=135)	100% (n=179)
pak-1	6.9% (n=187)	15.2% (n=131)
vab-19	5.5% (n=215)	16.1% (n=149)
unc-52	22% (n=263)	100% (n=195)
pat-3	47% (n=202)	49% (n=174)

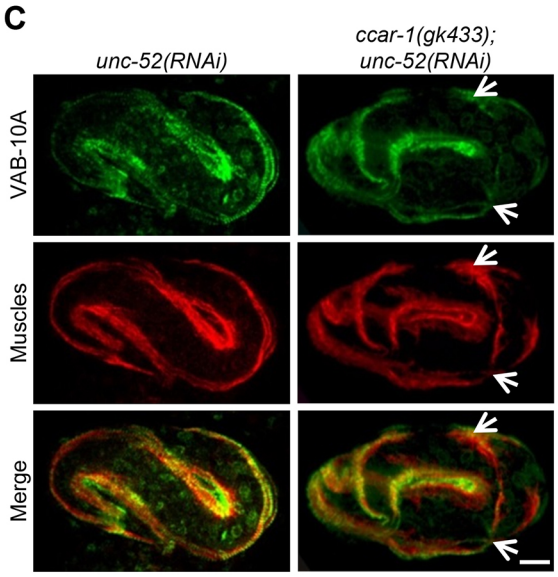

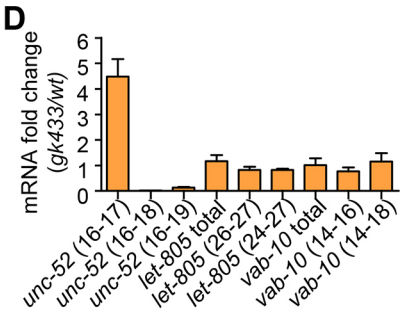

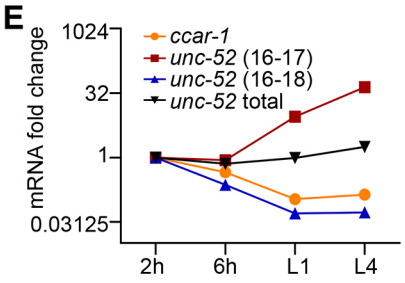

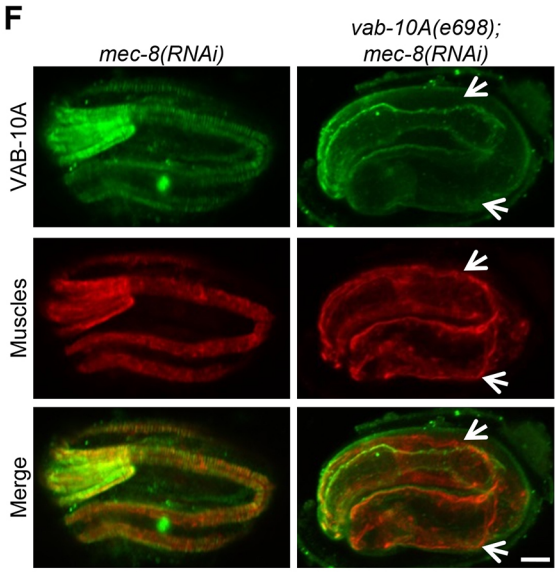

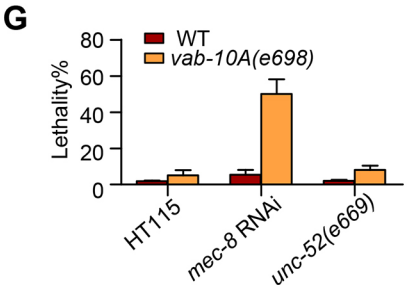

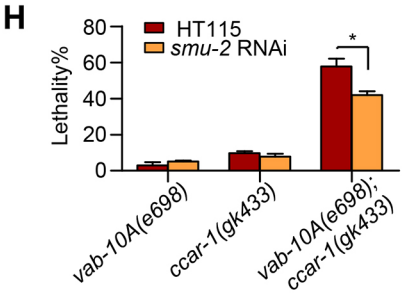

Fig. 3. CCAR-1 maintains CeHD integrity by regulating *unc-52* alternative splicing. (A) Results of QPCR experiments showing the transcription levels of CeHD-related components in *ccar-1(gk433)* embryos compared with wild type (WT) (three biological replicates, *n*>1000/condition). (B) Percentage of lethality in WT and *ccar-1(gk433)* animals treated with RNAi against CeHD-related genes. (C) VAB-10A (green) and PAT-3 (red) immunostaining of embryos treated with *unc-52* RNAi. Arrows, detached muscles. (D) Results of QPCR experiments showing the mRNA levels of *unc-52* isoforms containing exon 17 (16-17), skipping exon 17 (16-18), skipping exon 17 and 18 (16-19), and the alternative-spliced isoforms of *vab-10* and *let-805* in *ccar-1(gk433)* embryos compared with wild type (3 biological replicates, *n*>1000/condition). (E) Results of QPCR experiments showing the developmental changes of total *ccar-1*, *unc-52* isoforms containing exon 17 (16-17) and skipping exon 17 (16-18) and total *unc-52* in embryos at 2 h and 6 h of development and in L1 and L4 larvae. (F) VAB-10A (green) and PAT-3 (red) immunostaining of embryos treated with *mec-8* RNAi. Arrows, detached muscles. (G) Percentage lethality in WT, the *vab-10A(e698)* single mutant combined with control HT115 feeding, *mec-8* RNAi or *unc-52(e669)* mutation (three biological replicates, *n*≥75/condition). (H) Percentage lethality in mutants with or without *smu-2* RNAi treatment (three biological replicates, *n*≥68/condition). Error bars represent the s.e.m. **P*<0.05 (two-tailed unpaired *t*-test). Scale bars: 5 µm.

UNC-52 is the *C. elegans* homolog of mammalian perlecan and is an ECM protein produced mainly by epidermal cells (Rogalski et al., 1995; Spike et al., 2002). UNC-52 is distributed in the basal ECM, presumably binding to the basal CeHD receptor LET-805. Because the total transcription level of *unc-52* was unchanged upon loss of CCAR-1 function (Fig. 3A), we went on and examined the alternative splicing of the *unc-52* locus. Specifically, exons 16–19 of *unc-52*, which encode several immunoglobulin repeats, undergo a series of alternative splicing events that were frequently used as splicing reporters in previous works (Kabat et al., 2009; Lundquist et al., 1996; Rogalski et al., 1995; Spartz et al., 2004; Spike et al., 2001). However, the functional implications of *unc-52* alternative

splicing had not been determined. We found that the frequency of inclusion of *unc-52* exon 17 was dramatically elevated in *ccar-1(gk433)* embryos, while the excision frequency of exon 17 or exons 17–18 was significantly decreased (Fig. 3D). By contrast, the two other CeHD-related genes undergoing alternative splicing were not dramatically affected by loss of *ccar-1* (Fig. 3D). The developmental expression curves also showed that decreased exon 17 excision of *unc-52* coincided with the reduction of *ccar-1* expression, especially during embryonic elongation (Fig. 3E). These results together suggest that the excision of *unc-52* exon 17 is promoted by CCAR-1 during development.

To confirm whether CCAR-1 indeed maintains CeHDs by regulating alternative splicing, we created conditions under which the inclusion of *unc-52* exon 17 is favored by inactivating MEC-8, a splicing factor facilitating exon 17 excision (Lundquist et al., 1996). RNAi against *mec-8* combined with *vab-10A(e698)* led to the muscle detachment phenotype and caused similar level of embryonic lethality to that seen in the *vab-10A(e698);ccar-1(gk433)* mutant (Fig. 3F,G). Conversely, ablation of the *unc-52* exon-17-containing isoforms by introducing *unc-52(e669)*, a nonsense mutation in exon 17, did not affect embryonic development in the *vab-10A(e698)* background (Fig. 3G) (Rogalski et al., 1995). These observations suggest that elevated *unc-52* exon 17 inclusion in embryos is harmful to CeHD biogenesis. Consistent with the above data, decreasing the amount of exon-17-containing *unc-52* isoforms by knocking down *smu-2*, a splicing factor promoting exon 17 inclusion, partially rescued the embryonic lethality of *vab-10A(e698);ccar-1(gk433)* mutants (Fig. 3H) (Spartz et al., 2004). Taken together, we propose that dysregulated *unc-52* alternative splicing compromises CeHD integrity in *vab-10A(e698);ccar-1(gk433)* loss-of-function mutants.

CCAR-1 regulates alternative splicing by physically interacting with splicing factor HRP-2

To elucidate how CCAR-1 regulates alternative splicing, we first examined whether CCAR-1 affects the transcription of splicing factors known to control *unc-52* splicing (Kabat et al., 2009; Lundquist et al., 1996; Spartz et al., 2004; Spike et al., 2001). QPCR analysis showed that there was no significant difference in the transcription of *smu-1*, *smu-2*, *mec-8* or *hrp-2* between *ccar-1(gk433)* and wild type (Fig. 4A). This suggests that transcriptional regulation of splicing factors is not the primary mechanism employed by CCAR-1 to regulate alternative splicing. To determine whether CCAR-1 participates in *unc-52* splicing in a more direct manner, we performed immunoprecipitation mass spectrometry (IP-MS) to search for CCAR-1-binding partners (Table S3). From the IP-MS results, we identified HRP-2, a member of the heterogeneous nuclear ribonucleoprotein (hnRNP) family and a known splicing factor.

HRP-2 has been reported to promote the inclusion of exon 17 and 18 of *unc-52*, a function directly opposed to that of CCAR-1 (Kabat et al., 2009). We confirmed the physical interaction between HRP-2 and CCAR-1A by co-immunoprecipitation (co-IP) in mammalian 293T cells (Fig. 4B). In addition, CCAR-1A colocalized with HRP-2 in nuclei throughout embryonic development (Fig. 4D). High-resolution microscopy showed that CCAR-1 and HRP-2 shared similar distribution patterns within the nucleus. In comparison, the nuclear distribution of SMU-2, another *unc-52*-regulating splicing factor not identified by IP-MS, is distinct from that of CCAR-1 (Fig. 4E). Because CCAR-1 and HRP-2 exert antagonistic effects on *unc-52* exon 17 splicing, we predicted that the binding between CCAR-1 and HRP-2 might suppress the splicing activity of HRP-2. Hence, there could be aberrantly elevated splicing activity of HRP-2 in *ccar-1* mutants. Consistent with our hypothesis, attenuation of HRP-2 function by means of RNAi significantly rescued the embryonic lethality of *vab-10A(e698);ccar-1(gk433)* (Fig. 4C). Taken together, these results indicate that CCAR-1A forms a complex with splicing factor HRP-2 to suppress the inclusion of *unc-52* exon 17 during alternative splicing.

Disrupted alternative splicing causes VAB-10A disassociation from CeHDs

Finally, to explore the detailed mechanisms by which dysregulated alternative splicing of *unc-52* affects CeHD biogenesis, we simultaneously inactivated *mec-8* and *ccar-1* to further promote exon 17 inclusion. Interestingly, the synergistic effect of *mec-8* and *ccar-1* inactivation caused more than 50% embryonic lethality, accompanied by muscle detachment, suggesting that severe disruption of alternative splicing alone can compromise CeHD integrity (Fig. 4F, G). Furthermore, the localization of VAB-10A at CeHDs is greatly diminished in *ccar-1(gk433);mec-8(RNAi)* embryos (Fig. 4F). Consequently, intermediate filaments, which are normally attached to the CeHDs through VAB-10A association, became untethered and randomly scattered within the epidermis (Fig. 4F) (Zhang and Labouesse, 2010). In order to quantify the degree of VAB-10 dissociation from the CeHDs, we double-stained embryos with antibodies against VAB-10A and an internal staining control, AJM-1, as previously performed (Zahreddine et al., 2010). The results showed that the amount of VAB-10A at CeHDs was decreased by more than 50% when both *ccar-1* and *mec-8* were inactivated (Fig. 4H,I). It is worth noting that in *mec-8(RNAi)* or *ccar-1(gk433)* single mutants, the amount of VAB-10A at CeHDs was unchanged compared with that in wild type, indicating that *vab-10A* is not a direct target of alternative splicing (Fig. 4H,I). These observations suggest that severe disruption of *unc-52* alternative splicing causes dissociation of VAB-10A from CeHDs, possibly by affecting the binding affinity of VAB-10A to CeHD receptors indirectly through ligand–receptor interactions and protein conformational change.

To summarize, this work establishes CCAR-1 as a protein that stabilizes the CeHD through regulation of alternative splicing. Interestingly, of the 14 CeHD regulators identified in our previous screen, four have now turned out to be involved in alternative splicing (*ccar-1*, *unc-52*, *mec-8* and *hrp-1*) (Zahreddine et al., 2010). Similarly, nearly all genes encoding mammalian hemidesmosome-related components are alternatively spliced (Andrä et al., 2003; Buchroithner et al., 2004; Okumura et al., 2002; Sugaya et al., 2006). These findings reveal the previously unappreciated importance of alternative splicing in the dynamic process of hemidesmosome biogenesis.

It was believed that mammalian CCAR1 affects tumorigenesis mainly by regulating the transcription of genes involved in proliferation, apoptosis and differentiation (Kim et al., 2008; Muthu et al., 2015). Our discovery provides a novel insight into the cancer-related roles of CCAR1. Several recent works have tightened the links between hemidesmosomes and carcinogenesis (Cheung et al., 2016; De Arcangelis et al., 2016; Laval et al., 2014; Stewart and O'Connor, 2015). Moreover, most cancers affected by CCAR1 are derived from epithelial cells and occur in hemidesmosome-containing tissues (Muthu et al., 2015). The above facts increase the probability that CCAR1 affects the functional state of hemidesmosomes through alternative splicing during tumor progression. Last but not least, CCAR1 is an evolutionarily conserved gene expressed in most cell types. This means that CCAR1 could have a more general role in alternative splicing during multiple biological processes across species.

Journal of Cell Science (2018) 131, jcs214379. doi:10.1242/jcs.214379

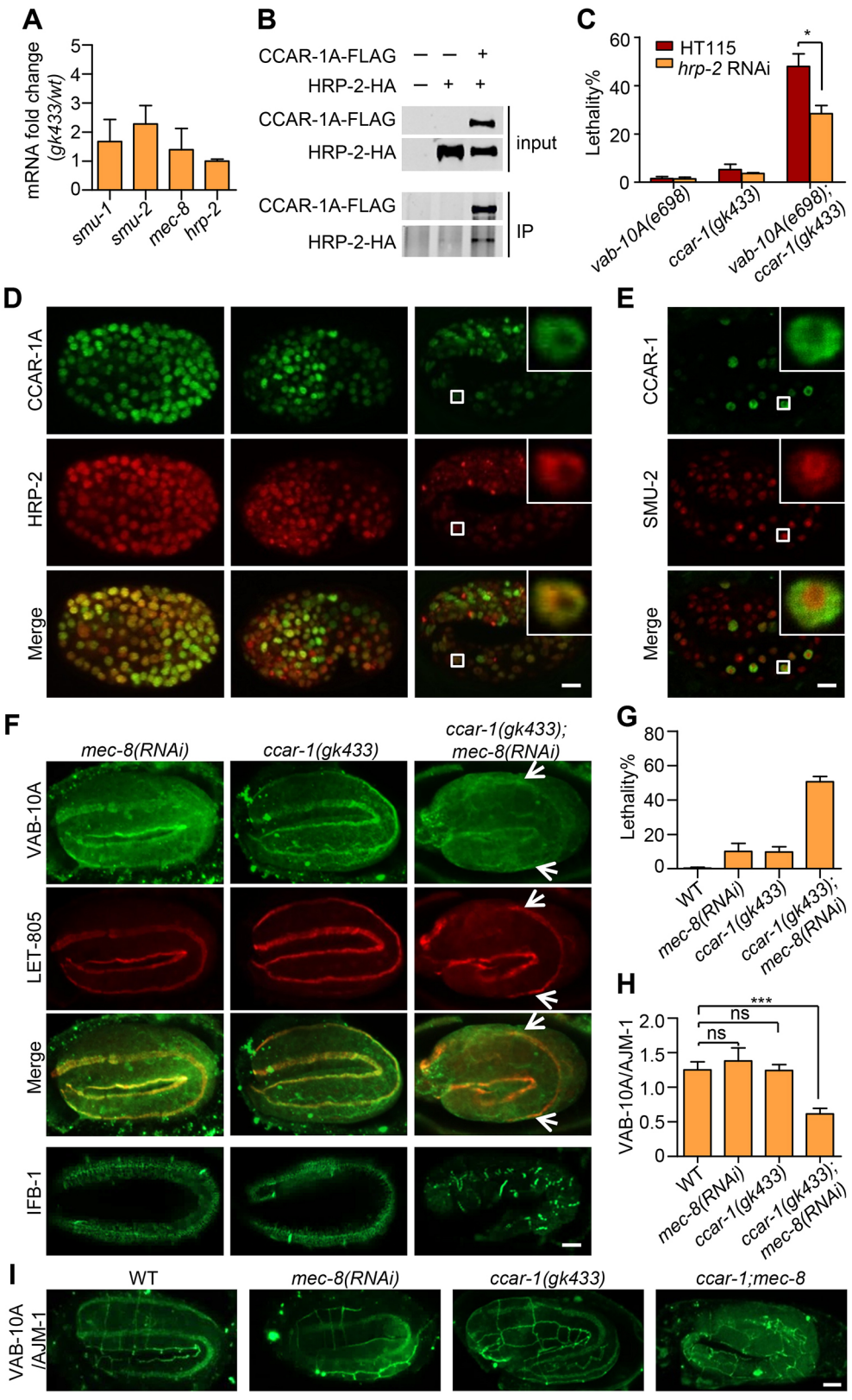

Fig. 4. CCAR-1 regulates alternative splicing by physically interacting with HRP-2 and stabilizes VAB-10A at CeHDs. (A) Results of QPCR experiments showing the transcription levels of *unc-52*-related splicing factors in *ccar-1(gk433)* embryos compared with wild type (three biological replicates, n>1000/condition). (B) Co-IP of CCAR-1A::FLAG and HRP-2::HA in 293T cells. (C) Lethality in mutants with or without *hrp-2* RNAi treatment (three biological replicates, $n\geq89$/condition). (D) CCAR-1A::GFP and HRP-2::mCherry colocalization in the gastrula, bean and 3-fold embryonic stages. (E) SMU-2::GFP and *dpy-7* promoter-driven CCAR-1::mCherry distribution in a three-fold embryo. Insets in D and E correspond to boxed areas in each image. (F) VAB-10A (green) and LET-805 (red) immunostaining and IFB-1::GFP distribution in *mec-8* RNAi, *ccar-1(gk433)* and *ccar-1(gk433); mec-8* RNAi mutant embryos. Arrows, detached muscles. (G) Percentage lethality in embryos with or without *mec-8* RNAi treatment (three biological replicates, n>100/condition). (H,I) VAB-10A and AJM-1 immunostaining and morphometric quantification of VAB-10A signals at CeHDs using AJM-1 as internal control ($n\geq10$/genotype). Error bars represent the s.e.m. *P<0.05; ***P<0.001; ns, not significant (two-tailed unpaired t-test). Scale bars: 5 µm.

MATERIALS AND METHODS

Worm strains and maintenance

Nematodes were maintained as previously described by Brenner at 20°C unless otherwise specified (Brenner, 1974). The strains N2, CB669, VC1029, CB698 and SP2533 were provided by the *Caenorhabditis* Genetics Center. Table S4 lists all the strains and full genotypes used in this study.

CRISPR/Cas9-mediated deletion of the *ccar-1* gene

The CRISPR-Cas9 vector (pDD162-Peft-3::CAS9-PU6) and protocol was kindly provided by the laboratory of Xiaochen Wang (IBP, Beijing, China). The sgRNA sequence targeting *ccar-1* exon 7 was designed via the online CRISPR design tool (http://crispr.mit.edu/). The optimized sgRNA sequence (5′-GGGAGCGGCGGTAAAATCATCGG-3′) was inserted into

the CRISPR-Cas9 vector using the Q5® site-directed mutagenesis kit (NEB, Ipswich, MA). Mutant strains were generated by microinjecting 50 ng/µl Cas9-*ccar-1* sgRNA plasmid with 50 ng/µl Cas9-*dpy-10* sgRNA plasmid, as a visual marker. The allele *sda11* with the small deletion (nucleotides 3059–3071 of CCAR-1A cDNA) plus a presumable frameshift was identified by PCR and sequencing. Four backcrosses to N2 were performed after obtaining the homozygous mutants.

RNAi and lethality analysis

The RNAi plasmid targeting *smu-2* was generated by cloning a 598 bp 3′ cDNA fragment of *smu-2* (amplified by primers: Forward 5′-AGGAAGTCGGCGGGATAG, Reverse 3′-CTCCGGCCTTCCGTTTAT) into L4440 vector. An 863 bp 3′ genomic fragment of *hrp-2* (amplified by primers: Forward 5′-CAACAATGGCTACGACATGC, Reverse 3′-GCTTTCCGTTGTCTCGTTTC) was used for the RNAi plasmid targeting *hrp-2*. Other RNAi clones were obtained from the MRC RNAi library and verified by sequencing. The plates seeded with RNAi bacteria were made as previously described (Kamath et al., 2003). Strains were fed with RNAi bacteria from the L1 stage together with control worms fed with HT115. For most RNAi experiments, worms grown into the adult stage with one row of eggs were allowed to lay eggs for 4 h on a fresh NGM plate and then removed. For knockdown of *hrp-2*, young adult mothers with only a few eggs were collected for egg-laying to avoid early embryonic lethality (Kinnaird et al., 2004). For RNAi against *mup-4*, *let-805* and *pat-3*, worms were fed with RNAi bacteria from the L3–L4 stage to prevent premature lethality of the mothers. The total numbers of eggs laid were counted and the lethality of the progenies was examined 24 h later if kept at 20°C or 48 h later if kept at 15°C.

Molecular biology and transgenesis

All fusion plasmids were constructed using the ClonExpressTM One Step Cloning Kit (Vazyme Biotech, Nanjing, China). The Pccar-1::CCAR-1A::gfp plasmid was created by inserting an 1602 bp *ccar-1* promoter and CCAR-1A cDNA into the pPD95.75 vector. The Pccar-1::ccar-1::gfp plasmid was constructed by cloning the genomic sequence of *ccar-1*, including the 1602 bp promoter and the entire coding sequence of *ccar-1*, into pPD95.75. The Pdpy-7::ccar-1::mCherry and Pdpy-7::CCAR-1A::mcherry plasmids were constructed by inserting a genomic fragment of the entire *ccar-1* coding sequence or CCAR-1A cDNA between 650 bp *dpy-7* promoter and mCherry into the pPD49.78 vector. The Phrp-2::hrp-2::mCherry construct was generated by inserting the *hrp-2* genomic fragment including 4004 bp promoter and 4047 bp coding sequence into the pPD49.78 vector. Microinjection was carried out as previously described to obtain transgenic worms (Zhang et al., 2015). The fusion constructs were injected at 10 ng/µl, along with 100 ng/µl pRF4 [*rol-6(su1006)*] or 20 ng/µl Pmyo-2::gfp as selection markers.

For mammalian cell culture and co-IP studies, CCAR-1A cDNA and HRP-2A cDNA were cloned into Pcmv::flag and Pcmv::HA vectors (gifts from Shuai Wang, IBMS, Soochow University, China), respectively. 293T cells were transfected with 1 µg/well of each plasmid using Lipofectamine 3000 (Life Technologies, Carlsbad, CA) when cells were about 80% confluent.

Immunostaining, fluorescence microscopy and image analysis

Embryos were fixed and stained for indirect immunofluorescence after freeze-cracking to remove the egg shell as described previously (Costa et al., 1997). The VAB-10A polyclonal antibody was raised by B&M BIOTECH (Beijing, China) against peptides CINWHGQPSELRNSQTDP and CGYKFRISEYDDSQAQRQ as described previously (Bosher et al., 2003). The MUP-4 polyclonal antibody was raised by Youke (Shanghai, China) against peptide PRAKLARPLYGDEMGDD as described previously (Hong et al., 2001). Monoclonal antibody MH25 (anti-PAT-3), MH46 (anti-LET-805), MH5 (anti-VAB-10A) and MH27 (anti-AJM-1) were obtained from DSHB (Iowa University, Iowa City, IA). The dilution factors for the primary antibodies are: anti-VAB-10A, 1:3500; MH25, 1:100; MUP-4, 1:500; MH46, 1:100; MH5, 1:50; MH27, 1:100. Alexa Fluor® 488- and Alexa Fluor® 568-labeled secondary antibodies (A-11008, A-11004 and A-11001, Molecular Probes, Eugene, OR, USA) were used at 1:800 dilution. For confocal imaging of immunostained animals or live animals expressing fluorescent reporters, stacks of images were captured every 1 µm using a Nikon A1 confocal microscope (Nikon, Tokyo, Japan) and processed with ImageJ (http://rsb.info.nih.gov/ij/).

Quantification of the VAB-10A signal in CeHD regions was performed as previously described (Zahreddine et al., 2010). For each experimental group, 10–12 embryos at about the two-fold stage were quantified using ImageJ software (http://rsb.info.nih.gov/ij). For body length measurement, bright-field images of *vab-10A(e698)*, *ccar-1(gk433)*, and *vab-10A(e698); ccar-1(gk433)* adult stage worms were captured with an Olympus SZX16 stereo microscope (Olympus, Tokyo, Japan) and the body length of each adult was measured using ImageJ software (http://rsb.info.nih.gov/ij/) as previously described (Zhang et al., 2011).

Microarray and QPCR analysis

For microarray analysis, bleached wild-type or *ccar-1(gk433)* mutant embryos were allowed to develop in M9 for 6 h to obtain elongation stage embryos. Total RNA was isolated by using the RNeasy microarray tissue mini kit (QIAGEN, Hilden, Germany). For each genotype, three individual replicates were performed and RNA was hybridized to Affymetrix *C. elegans* Genechips (Thermo Fisher Scientific, Carlsbad, CA). Microarray analysis and data processing was performed by the Microarray and Sequencing Platform at the Institut de Génétique et de Biologie Moléculaire et Cellulaire (IGBMC). All data can be downloaded from supplementary table (Table S2).

For developmental gene expression analysis, embryos were collected in M9 buffer by bleaching mothers with one row of eggs and were then incubated at 20°C for 2 h or 6 h. L1 stage worms were generated by hatching embryos in M9 buffer. Synchronized L1 worms were fed with *Escherichia coli* OP50 for 48 h to obtain L4 stage worms. For other QPCR experiments, bleached embryos were allowed to develop in M9 for 6 h to obtain elongation stage embryos. Total RNA was isolated with TRIzol reagent (TakaRa, Otsu, Shiga, Japan) and reverse transcribed into cDNA by using the PrimeScript RT Master Mix (TakaRa, Otsu, Shiga, Japan). To specifically amplify the *unc-52* 16-18 isoform (skipping exon 17), the cDNA was digested with the restriction enzyme AccI, targeting exon 17, overnight before QPCR to avoid the PCR amplification of the *unc-52* 16-17-18 band. FastStart Universal SYBR Green Master Mix (Roche, Mannheim, Germany) was used to set up the QPCR in a Mastercycler EP realplex machine (Eppendorf, Hamburg, Germany). At least three RNA samples were tested for each experiment and each reaction was run in quadruplicate. *tba-1* was used as the internal reference gene to analyze the change of mRNA level in embryos. In the gene expression analysis, Y45F10D.4 was used as the reference gene. All results were analyzed with REST 2009 software (QIAGEN). Primers used for QPCR are listed in Table S5.

IP-MS and co-IP

The strain HMZ0081 [*ccar-1(gk433)*;sdaEx26(P*ccar-1*::*ccar-1*::GFP +pRF4)] was used for IP-MS analysis. Mixed stage worms were cultured on 100 mm NGM plates and washed off the plates by using M9 buffer. After three washes, the samples were centrifuged at 1730 ***g*** for 1 min to remove the supernatant. A 2 ml volume of worm pellets were stored in liquid nitrogen until sending for IP-MS analysis. The sample treatment, IP-MS procedure and data analysis was performed essentially as previously described (Yang et al., 2017; Zhu et al., 2015).

293T cells plated on a six-well plate (Corning Life Sciences, Tewksbury, MA) were transfected with 1 µg/well of each plasmid using Lipofectamine 3000 (Life Technologies, Carlsbad, CA, USA) when cells were about 80% confluent. Transfected cells were collected after 48 h incubation. co-IP was performed following the manufacturer's protocol using the Pierce Crosslink Immunoprecipitation Kit (Thermo Fisher Scientific, Rockford, IL, USA). 2 µg/µl precleared cell lysates was incubated with rabbit anti-FLAG (1:50, F7425, Sigma-Aldrich, St Louis, MO) at 4°C overnight, followed by incubation with protein A/G plus agarose at room temperature (RT) for 1 h. The immunoprecipitated complex was washed three times with lysis buffer and re-suspended in 1× loading buffer and then boiled at 95°C for 5 min for SDS-PAGE analysis.

For western blotting of proteins from the co-immunoprecipitation analysis, a 7.5% SDS-PAGE gel was used to separate input and immunoprecipitated proteins. Mouse anti-FLAG (1:5000, M20008, Abmart, Berkeley Heights, NJ, US) and anti-HA (1:4000, ab9110,

Abcam, Cambridge, UK) were used as primary antibodies and IRDye 800CW (1:5000,926-32210, LI-COR, Lincoln, NE, USA) as the secondary antibody. The Odyssey SA imaging system (LI-COR) was used for visualizing the western blot results.

Statistical analysis

Statistical analysis was performed using GraphPad Prism 5.0 software. A two-tailed unpaired *t*-test was used to calculate statistical significance, as described in the figure legends.

Acknowledgements

We thank Robert Herman, Shiqing Cai, Hui Zheng and the *Caenorhabditis* Genetics Center for reagents, and Hala Zahreddine, Sandrine Hild and Shuai Wang for technical support. The *Caenorhabditis* Genetics Center is funded by National Institutes of Health National Center for Research Resources (P40 OD010440).

Competing interests

The authors declare no competing or financial interests.

Author contributions

Conceptualization: R.F., M.L., H.Z.; Methodology: R.F., M.D., H.Z.; Validation: Y.Z., X.J., Y.L.; Formal analysis: R.F., Y.Z., X.J.; Investigation: R.F., Y.Z., X.J., Y.L., M.Z., Z.H., C.W., H.Z.; Resources: R.F., Y.Z.; Data curation: R.F., Y.Z., M.Z., H.Z.; Writing - original draft: R.F.; Writing - review & editing: M.L., H.Z.; Visualization: R.F., Y.Z., X.J., Y.L.; Supervision: H.Z.; Project administration: H.Z.; Funding acquisition: M.L., H.Z.

Funding

This work was supported by the National Natural Science Foundation of China [31271429, 31471265 and 31670912], a Jiangsu Provincial Distinguished Young Scholars award [BK20160009], the Jiangsu Provincial Innovative Research Team, the Program for Changjiang Scholars and Innovative Research Team in University (PCSIRT) [IRT1075] and the Priority Academic Development Program of Jiangsu Province Higher Education Institutions (PAPD) to H.Z., and by the Israel-France Maimonides program, the French Agence Nationale de la Recherche and the European Union to M.L.

Supplementary information

Supplementary information available online at
http://jcs.biologists.org/lookup/doi/10.1242/jcs.214379.supplemental

References

Andrä, K., Kornacker, I., Jörgl, A., Zörer, M., Spazierer, D., Fuchs, P., Fischer, I. and Wiche, G. (2003). Plectin-isoform-specific rescue of hemidesmosomal defects in plectin (-/-) keratinocytes. *J. Invest. Dermatol.* **120**, 189-197.

Bosher, J. M., Hahn, B.-S., Legouis, R., Sookhareea, S., Weimer, R. M., Gansmuller, A., Chisholm, A. D., Rose, A. M., Bessereau, J. L. and Labouesse, M. (2003). The Caenorhabditis elegans vab-10 spectraplakin isoforms protect the epidermis against internal and external forces. *J. Cell Biol.* **161**, 757-768.

Brenner, S. (1974). The genetics of Caenorhabditis elegans. *Genetics* **77**, 71-94.

Brunquell, J., Yuan, J., Erwin, A., Westerheide, S. D. and Xue, B. (2014). DBC1/CCAR2 and CCAR1 are largely disordered proteins that have evolved from one common ancestor. *Biomed. Res. Int.* **2014**, 418458.

Buchroithner, B., Klausegger, A., Ebschner, U., Anton-Lamprecht, I., Pohla-Gubo, G., Lanschuetzer, C. M., Laimer, M., Hintner, H. and Bauer, J. W. (2004). Analysis of the LAMB3 gene in a junctional epidermolysis bullosa patient reveals exonic splicing and allele-specific nonsense-mediated mRNA decay. *Lab. Invest.* **84**, 1279-1288.

Cheung, K. J., Padmanaban, V., Silvestri, V., Schipper, K., Cohen, J. D., Fairchild, A. N., Gorin, M. A., Verdone, J. E., Pienta, K. J., Bader, J. S. et al. (2016). Polyclonal breast cancer metastases arise from collective dissemination of keratin 14-expressing tumor cell clusters. *Proc. Natl. Acad. Sci. USA* **113**, E854-E863.

Costa, M., Draper, B. W. and Priess, J. R. (1997). The role of actin filaments in patterning the Caenorhabditis elegans cuticle. *Dev. Biol.* **184**, 373-384.

De Arcangelis, A., Hamade, H., Alpy, F., Normand, S., Bruyere, E., Lefebvre, O., Mechine-Neuville, A., Siebert, S., Pfister, V., Lepage, P. et al. (2016). Hemidesmosome integrity protects the colon against colitis and colorectal cancer. *Gut.* **66**, 1748-1760.

Ha, S. Y., Kim, J. H., Yang, J. W., Kim, J., Kim, B. and Park, C.-K. (2016). The overexpression of CCAR1 in hepatocellular carcinoma associates with poor prognosis. *Cancer Res. Treat* **48**, 1065-1073.

Hong, L., Elbl, T., Ward, J., Franzini-Armstrong, C., Rybicka, K. K., Gatewood, B. K., Baillie, D. L. and Bucher, E. A. (2001). MUP-4 is a novel transmembrane protein with functions in epithelial cell adhesion in Caenorhabditis elegans. *J. Cell Biol.* **154**, 403-414.

Kabat, J. L., Barberan-Soler, S. and Zahler, A. M. (2009). HRP-2, the Caenorhabditis elegans homolog of mammalian heterogeneous nuclear ribonucleoproteins Q and R, is an alternative splicing factor that binds to UCUAUC splicing regulatory elements. *J. Biol. Chem.* **284**, 28490-28497.

Kamath, R. S., Fraser, A. G., Dong, Y., Poulin, G., Durbin, R., Gotta, M., Kanapin, A., Le Bot, N., Moreno, S., Sohrmann, M. et al. (2003). Systematic functional analysis of the Caenorhabditis elegans genome using RNAi. *Nature* **421**, 231-237.

Kim, J. H., Yang, C. K., Heo, K., Roeder, R. G., An, W. and Stallcup, M. R. (2008). CCAR1, a key regulator of mediator complex recruitment to nuclear receptor transcription complexes. *Mol. Cell* **31**, 510-519.

Kinnaird, J. H., Maitland, K., Walker, G. A., Wheatley, I., Thompson, F. J. and Devaney, E. (2004). HRP-2, a heterogeneous nuclear ribonucleoprotein, is essential for embryogenesis and oogenesis in Caenorhabditis elegans. *Exp. Cell Res.* **298**, 418-430.

Laval, S., Laklai, H., Fanjul, M., Pucelle, M., Laurell, H., Billon-Galés, A., Le Guellec, S., Delisle, M. B., Sonnenberg, A., Susini, C. et al. (2014). Dual roles of hemidesmosomal proteins in the pancreatic epithelium: the phosphoinositide 3-kinase decides. *Oncogene* **33**, 1934-1944.

Litjens, S. H. M., de Pereda, J. M. and Sonnenberg, A. (2006). Current insights into the formation and breakdown of hemidesmosomes. *Trends Cell Biol.* **16**, 376-383.

Lu, C.-K., Lai, Y.-C., Lin, Y.-F., Chen, H.-R. and Chiang, M.-K. (2012). CCAR1 is required for Ngn3-mediated endocrine differentiation. *Biochem. Biophys. Res. Commun.* **418**, 307-312.

Lundquist, E. A., Herman, R. K., Rogalski, T. M., Mullen, G. P., Moerman, D. G. and Shaw, J. E. (1996). The mec-8 gene of C. elegans encodes a protein with two RNA recognition motifs and regulates alternative splicing of unc-52 transcripts. *Development* **122**, 1601-1610.

Muthu, M., Cheriyan, V. T. and Rishi, A. K. (2015). CARP-1/CCAR1: a biphasic regulator of cancer cell growth and apoptosis. *Oncotarget* **6**, 6499-6510.

Okumura, M., Yamakawa, H., Ohara, O. and Owaribe, K. (2002). Novel alternative splicings of BPAG1 (bullous pemphigoid antigen 1) including the domain structure closely related to MACF (microtubule actin cross-linking factor). *J. Biol. Chem.* **277**, 6682-6687.

Ou, C.-Y., Kim, J. H., Yang, C. K. and Stallcup, M. R. (2009). Requirement of cell cycle and apoptosis regulator 1 for target gene activation by Wnt and beta-catenin and for anchorage-independent growth of human colon carcinoma cells. *J. Biol. Chem.* **284**, 20629-20637.

Rogalski, T. M., Gilchrist, E. J., Mullen, G. P. and Moerman, D. G. (1995). Mutations in the unc-52 gene responsible for body wall muscle defects in adult Caenorhabditis elegans are located in alternatively spliced exons. *Genetics* **139**, 159-169.

Spartz, A. K., Herman, R. K. and Shaw, J. E. (2004). SMU-2 and SMU-1, Caenorhabditis elegans homologs of mammalian spliceosome-associated proteins RED and fSAP57, work together to affect splice site choice. *Mol. Cell. Biol.* **24**, 6811-6823.

Spike, C. A., Shaw, J. E. and Herman, R. K. (2001). Analysis of smu-1, a gene that regulates the alternative splicing of unc-52 pre-mRNA in Caenorhabditis elegans. *Mol. Cell. Biol.* **21**, 4985-4995.

Spike, C. A., Davies, A. G., Shaw, J. E. and Herman, R. K. (2002). MEC-8 regulates alternative splicing of unc-52 transcripts in C. elegans hypodermal cells. *Development* **129**, 4999-5008.

Stewart, R. L. and O'Connor, K. L. (2015). Clinical significance of the integrin alpha6beta4 in human malignancies. *Lab. Invest.* **95**, 976-986.

Sugaya, K., Hongo, E., Ishihara, Y. and Tsuji, H. (2006). The conserved role of Smu1 in splicing is characterized in its mammalian temperature-sensitive mutant. *J. Cell Sci.* **119**, 4944-4951.

Yang, Y., Zhang, Y., Li, W. J., Jiang, Y., Zhu, Z., Hu, H., Li, W., Wu, J. W., Wang, Z. X., Dong, M. Q. et al. (2017). Spectraplakin induces positive feedback between fusogens and the actin cytoskeleton to promote cell-cell fusion. *Dev. Cell* **41**, 107-120 e4.

Zahreddine, H., Zhang, H., Diogon, M., Nagamatsu, Y. and Labouesse, M. (2010). CRT-1/calreticulin and the E3 ligase EEL-1/HUWE1 control hemidesmosome maturation in C. elegans development. *Curr. Biol.* **20**, 322-327.

Zhang, H. and Labouesse, M. (2010). The making of hemidesmosome structures in vivo. *Dev. Dyn.* **239**, 1465-1476.

Zhang, H., Landmann, F., Zahreddine, H., Rodriguez, D., Koch, M. and Labouesse, M. (2011). A tension-induced mechanotransduction pathway promotes epithelial morphogenesis. *Nature* **471**, 99-103.

Zhang, Y., Li, W., Li, L., Li, Y., Fu, R., Zhu, Y., Li, J., Zhou, Y., Xiong, S. and Zhang, H. (2015). Structural damage in the C. elegans epidermis causes release of STA-2 and induction of an innate immune response. *Immunity* **42**, 309-320.

Zhu, M., Wu, G., Li, Y. X., Stevens, J. K., Fan, C. X., Spang, A. and Dong, M. Q. (2015). Serum- and glucocorticoid-inducible kinase-1 (SGK-1) plays a role in membrane trafficking in Caenorhabditis elegans. *PLoS One* **10**, e0130778.